Fuel 209 (2017) 265–273

Contents lists available at ScienceDirect

Fuel

journal homepage: www.elsevier.com/locate/fuel

Full Length Article

Experimental study of Polycyclic Aromatic Hydrocarbons (PAHs) in n-Heptane laminar diffusion flames from1.0 to 3.0 bar

Lei Zhou[a], Gaihua Xiong[a], Mengjie Zhang[a], Longfei Chen[b,*], Shirun Ding[b], L.P.H. de Goey[c]

[a] School of Mechanical Engineering and Automation, Harbin Institute of Technology (Shenzhen), 518055 Shenzhen, Guangdong, China
[b] School of Energy and Power Engineering, Energy and Environment International Center, Beihang University, 100191 Beijing, China
[c] Department of Mechanical Engineering, Eindhoven University of Technology (TU/e), P.O. Box 513, 5600 MB Eindhoven, The Netherlands

ARTICLE INFO

Keywords:
Laminar diffusion flames
PAHs
Soot
n-heptane
Elevated pressure
LIF
LII

ABSTRACT

As PAHs (Polycyclic Aromatic Hydrocarbons) are the main precursor of soot formation during the combustion, the investigation of PAHs formation is essential for the understanding of the soot formation and soot reduction in combustion. In this study, a specially designed burner and the corresponding fueling system was used to stabilize a laminar diffusion flame of n-heptane up to 3.0 bar before it becomes unstable. Using the combination of LII (Laser Induced Incandescence) and LIF (Laser Induced Fluorescence) techniques, the PAHs and soot formation and their distributions in the studied flames were obtained and explained. The results showed that PAHs were almost surrounded by soot and were present in the lower part of the flame. Moreover, the integral soot and PAH intensities exhibited a power law dependence on the pressure, being proportional to p^n with n of 1.38 ± 0.32 and 1.49 ± 0.25 respectively under the pressure range of 1.0–3.0 bar.

1. Introduction

Polycyclic Aromatic Hydrocarbons (PAHs) are toxic organic chemicals generated during incomplete combustion from numerous mobile, industrial, agricultural, domestic, and natural sources [1]. They pose a serious threat to health because they are ubiquitous and toxic [2]. PAHs are also the precursor of soot formation in combustion which is one of the pollutants that could severely deteriorate air quality. When the fuel has aromatic ingredients, the formation of PAHs becomes intense in combustion, particularly at elevated pressure. While most practical combustion systems work at high pressure, little work has been experimentally performed on the effect of pressure on the PAHs formation, which may be due to the challenges in stabilizing sooting flames at high pressures, even for laminar diffusion flames that are good targets to investigate the effects of pressure on PAHs formation.

The combustion of transportation fuels, such as diesel, contribute significantly to the PAHs emissions. Liu et al. [2] pointed out that one of the measures to reduce PAHs emissions in the future would be to control emissions of diesel engines. The composition of diesel, however, is relatively complex, therefore n-heptane is considered as a diesel surrogate because of its approximate Cetane Number [3]. Therefore, the study of n-heptane flames at elevated pressure can advance our understanding of the mechanism of PAHs formation in diesel combustion, in turn to mitigate PAHs and soot emissions.

Vander Wal [4] from NASA-Lewis Research Center found a decrease in LIF (Laser Induced Fluorescence) and the onset in the LII (Laser Induced Incandescence) signal at 33–34 mm HAB (Height Above Burner) in a laminar ethylene diffusion flame at atmospheric pressure. It pointed out that the entire soot formation process may be visualized from fuel pyrolysis regions containing PAHs with their subsequent condensation, coagulation, and carbonization leading to soot. Eaves et al. [5] conducted a numerical study for ethane–air co-flow diffusion flames at pressures from 2.0 to 15.0 bar. They pointed out that soot formation along the wings was seen to be surface growth dominated and PAHs condensation dominates centerline soot formation. For a better understanding of the PAHs formation process in co-flow flames, the mechanism of PAHs formation in methane and ethylene flame was studied by Slavinskaya [6]. The experiment was performed under atmospheric and pressurized conditions, and a dynamic mechanism which was relatively short and had a great significance for the explanation of the formation of PAHs and soot was developed. Moreover, they pointed out that high temperature reactions at elevated pressure had a large contribution on the formation of PAHs. Ethylene [7,8], methane [7,9–11], ethane[11,12] and propane flames [13] have been

Abbreviations: HAB, height above the burner; H_{mb}, height of the brightest point; H_{mbp}, mean height of brightest point in PAHs signals; $H_{mean\text{-}flame}$, mean height of the flame; I_{LIF}, intensity of the PAH-LIF signals; $I_{LIF\,\&\,LII}$, intensity of signals; I_{LII}, intensity of the soot formation signals; LIF, laser induced fluorescence; LII, laser induced incandescence; $W_{mean\text{-}flame}$, mean width of the flame; W_{ml}, width of the soot formation signals; W_{mp}, mean width of the PAHs signals

* Corresponding author.
E-mail address: chenlongfei@buaa.edu.cn (L. Chen).

http://dx.doi.org/10.1016/j.fuel.2017.07.074
Received 11 June 2017; Received in revised form 16 July 2017; Accepted 18 July 2017

investigated in laminar diffusion flames at high pressures. They focused on the formation of soot, yet few paid attention to the PAHs formation. In addition, these researches have only used gaseous fuels in laminar diffusion flames.

In order to extend the investigations into the liquid fuels, many researchers tried to study gaseous fuels doped with liquid fuels. Bejaoui et al. [14] analyzed the LIF signal of the PAHs formed in ethylene diffusion flames and premixed flames of diesel at the atmospheric condition, and the excitation properties of different PAHs components in the flame were investigated using lasers of different wavelengths. It was speculated that rubicene ($C_{26}H_{14}$) and its derivatives may form the first solid nuclei and eventually evolve to soot. Moreover, it was reported that the laser of 532 nm wavelength would excite large PAHs mainly and fluorescence signals are mainly obtained from them. Although the experiment involved liquid fuels, the experiment was still at atmospheric pressure. Daca et al.[15] carried out experiments to investigate the soot formation characteristics of diffusion flames of methane doped with toluene and n-heptane up to 6.0 bar and 8.0 bar respectively. They found that the flames of methane doped with toluene had a stronger tendency to product soot and were less sensitive to pressure, while PAHs formation was largely ignored.

A number of experiments of liquid fuels were also conducted, while most of them were at atmospheric pressure. Oliveira et al. [16,17] combined LII and LIF methods to conduct the measurement of liquid fuels, n-heptane and n-decane at atmospheric pressure, and the results indicated that the maximum PAH-LIF signal was a good predictor of maximum volume fraction of soot obtained from the LII signal. It was found that there was a linear correlation between the volume fraction of soot and the PAH-LIF and delayed LII signals (50 ns). Viteri et al. [18] conducted the experiments of pyrolysis of dimethyl carbonate at around atmospheric pressure. The toxicity of PAHs arouses their attention. They found that the PAHs had maximum production at 1375 K and PAHs would be greatly absorbed by soot at 1375 K and 1425 K. Although the experimental objects changed from the gaseous fuel to liquid fuels, the study was confined to atmospheric pressure. An et al. [19] analyzed their experimental and simulated results comprehensively and pointed out that large PAHs (A4-A6) are the key precursor of soot generated in GDI engines and they had a greater possibility of evolving to soot compared with small PAHs.

In summary, previous researches about soot and PAHs formations on laminar diffusion flames were either limited to gaseous fuels (and gaseous fuels doped with a small amount of liquid fuels), or limited to liquid fuels at atmospheric conditions (or liquid fuels at elevated pressures but only on the studies on soot formations). Consequently, the details about the PAHs formation in laminar diffusion flames of liquid fuels at elevated pressures need to be investigated more extensively. It is not only important for the explorations of the PAHs formation mechanisms, but also facilitates the exploration of suitable solutions towards reducing soot emissions in practical combustion equipment (e.g. automobile engines). However, due to the instabilities of the laminar diffusion flames of the liquid fuel while the pressure increases, most of previous studies have been focused on gaseous fuels [4–13]. Experimental studies of PAHs formation on laminar diffusion flames of liquid fuels under elevated pressures are rarely found in the literature.

In this study, a specially designed High Pressure Vessel Burner (HPVB) and the corresponding fueling system was used to investigate the PAHs formation in laminar diffusion flames of the liquid fuels at elevated pressures. The flame was stabilized up to 3.0 bar and the PAHs formation of laminar diffusion flames of n-heptane was measured with LIF by a 532 nm wavelength laser.

2. Materials and methods

2.1. High pressure vessel and burner (HPVB)

The burner test rig and the corresponding fueling system were illustrated in details in [3]. The flue gas from the exhaust of the pressure vessel has a temperature above 200 °C and is cooled before it passes through the pressure regulator. The pressure regulator of the pressure vessel and the pressure regulator of the liquid fuel accumulator are coupled, in order to keep the pressure in the accumulator at a higher level than the pressure in the vessel.

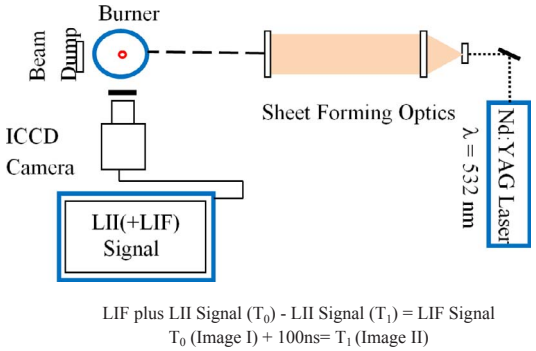

Fig. 1. Schematic diagram of the measurement set-up.

N-heptane is chosen as a surrogate fuel as it is one of the primary reference fuels for octane number evaluation [3]. Moreover, it is a representative component for the aliphatic fraction in commercial gasoline and diesel fuels.

2.2. Optical detection

The optical detection setup is shown in Fig. 1 and also presented in [3]. The laser is a Nd: YAG laser (one cavity of a Quantal Brio Twins system) operating at 532 nm. The energy is equal to 0.78 mJ/pulse. The prompt LII signal was collected by an intensified CCD camera (Princeton Instruments ICCD), using the prompt technique; a gate time of 100 ns was used, with the intensifier at a fixed gain and fully open upon arrival of the laser pulse. The raw LII images were averaged and corrected by subtracting luminescence signals [20,21]. The LII radiation was focused onto the ICCD using an f/2.8: 50 mm lens.

The experimental devices for detecting the LIF signal are the same with the apparatuses for detecting the LII signal mentioned in [3]. Under the condition of the same stable flame, the flame is excited by the laser. Actually, there are contributions from both soot-LII and PAH-LIF in the detected signal when the laser is on, see Fig. 1. Prompt detection by the ICCD (synchronized with the laser pulse) contains both LIF and LII contributions, but the delayed detection (100 ns after the power off of the laser pulse) avoids the LIF signals from PAHs due to their short life time (the longest time is less than 80 ns [22]). Therefore, one could obtain two-dimensional pictures including only the PAH-LIF signal after subtraction of the two signals. Although the measurements contain some incandescence, it turned out to be negligible compared to the PAHs signal [23]. Illustrated, at each measurement, the LIF plus LII signal image was captured by ICCD at T_0 (Image I), and the sole LII signal image (Image II) was captured by ICCD at T_1 (100 ns delay after the laser is turned off) while the fluorescence signals of PAHs in the flame was extinguished. As a result, the net LIF signal of PAHs can be obtained by a subtraction of signal of Image II from Image I

2.3. Measurement process

During the measurement, the fuel flow rate of n-heptane was kept at 6.0 g/h (1.67 mg/s), and the air co-flow was kept at 4.67 g/s with fixed supply pressure of 8 bar. The carrier nitrogen was maintained at 14 mg/s with a fixed supply pressure of 10 bar. The mass flow fraction of fuel in the fuel mixture including nitrogen carrier gas was 11%. Consequently, as the boiling point of n-heptane is 99 °C at 1 bar, the system temperature was kept at 180 °C which is enough to guarantee

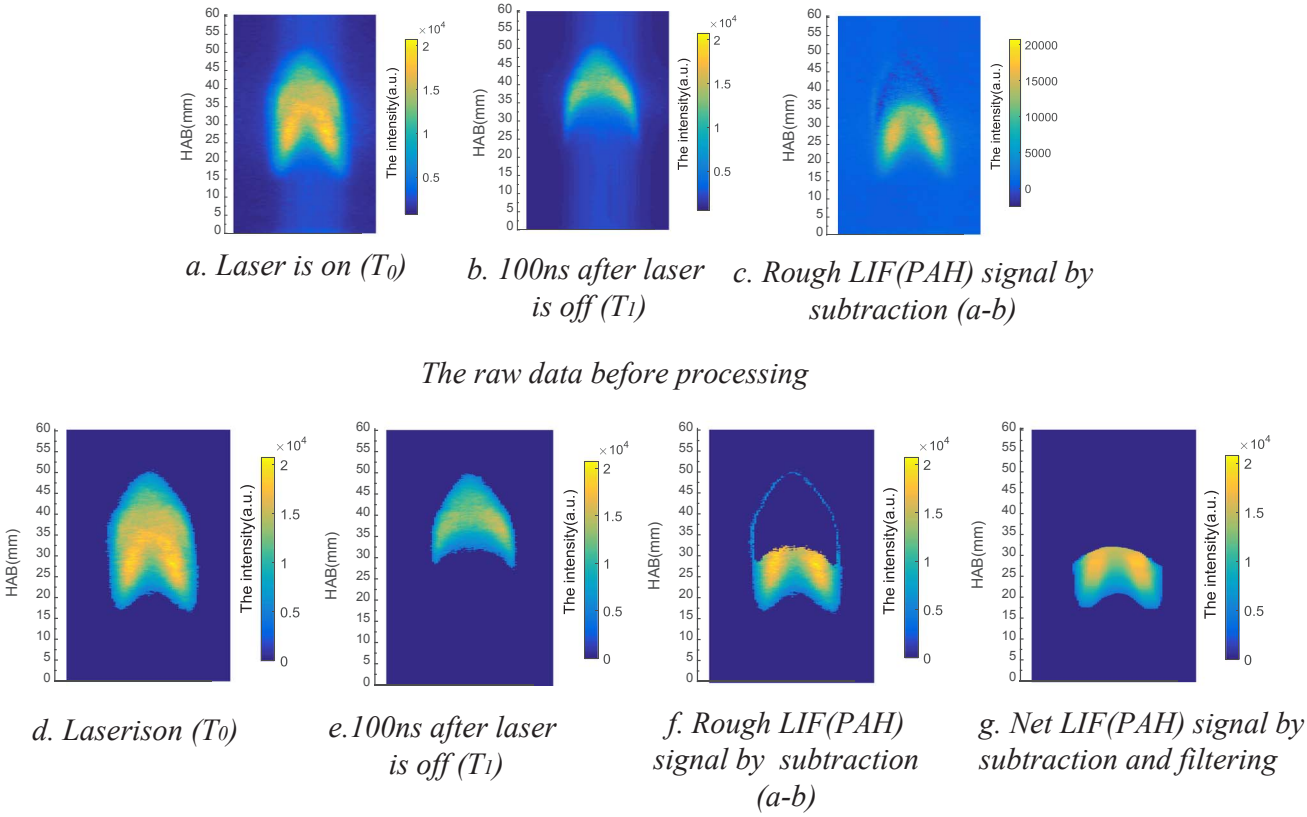

Fig. 2. PAHs (LIF) formation image processing (at 2.0 bar).

full evaporation of n-heptane. The mass flow rate of the fuel mixture in the tube and the co-flow around the tube were 1.25 mg/mm^2 s and 2.41 mg/mm^2 s, respectively. The ambient pressure in the vessel was varied from 1 bar to 3 bar.

Actually, the LII signal is also gradually attenuated with time, so the intensity of the LII signal at the same area at T_1 will not be completely equal to the LII signal at T_0. The LII signal cannot be eliminated by a simple subtraction so that there are some LII signals will be wrongly kept in the rough LIF signals (T_0-T_1). Accordingly, a correction for filtering off the remained LII signals will be adopted for obtaining a net LIF-PAHs image.

2.4. LIF signals (PAH) image processing

In this experiment, the laser passed through the flame, resulting in the components exited in the flame to emit light. They are recorded by the ICCD, then the LIF signal is expected by subtraction mentioned above. Effected by the function of the ICCD and the other experimental conditions, the raw experimental data is noisy. An obvious light beam (see Fig. 2) which does not belong to the flame and would affect the calculation of LII and LIF signals.

The signal to noise ratio of the flame data at 2.0 bar was 0.35, which was really large. In order to extract the real information, de-noising is processed. The values of the pixels on the edge of the flame in the images recorded by LII or LIF have been found, S_T. Then the value of the pixel in the image less than S_T has been eliminated and the pixels left are considered to record the intensity of the LII or LIF signals due to the fact that the luminance in the center of the flame is stronger than that in the edge of the flame. The signal to noise ratio raise up to 4.29 by the de-noising process.

Fig. 2d and e demonstrated an example of the measurement data at the pressure of 2.0 bar, and Fig. 2f was interpreted as the rough LIF signal, which was filtered to damp the noise. Fig. 2g is considered to be the real LIF signal.

The soot in the marginal area of the wing of the flame was attenuated faster than soot in the centerline of the flame due to their position in the large temperature gradient. The area of the LII signal at T_1 was smaller than the area of the LII signal at T_0. As a result, a simple area subtraction could not remove the whole LII signal so that the remained LII appeared as an “aureole” in the marginal area of the flame (see Fig. 2f). Eventually, as shown in Fig. 2g, the net LIF (PAHs) signal was carried out by the filtering process. The center flame was surrounded by a flame front, which led to the absence of the oxidative species in the center of the flame. The PAHs formation is the main reaction pathways for flame intermediates of soot [11] and the soot formation is dominated by PAHs condensation [5]. The main LIF signals of PAHs were captured with some negligible minor errors.

3. Results and discussions

3.1. Flame stability

This experiment utilized the same burner and fueling system as described in [3] which greatly enhances the uniformity of the temperature in the fueling system as well as the flame stability at elevated pressure. Nevertheless, the gas density and the buoyancy are scaled with pressure [7], the flame is more susceptible to buoyancy in a pressurized environment. Flame flickering and oscillations will increase with pressure, but the flame is sufficiently stable for soot measurement in laminar diffusion flames of n-heptane up to 3 bar on the condition that the standard deviation of the height of the flame based on 5 replicas is less than 1.6 mm (3% of the height of the flame). Unfortunately, when the pressure exceeds 3 bar, the flame seems to start rotating and pulsating. Further increasing pressure magnifies these instabilities. The flame rotation speed increases and rotating cells start in the flame base and grow towards the flame tip until they break the flame into sooting tips.

The oscillations in vertical and horizontal directions of the flames

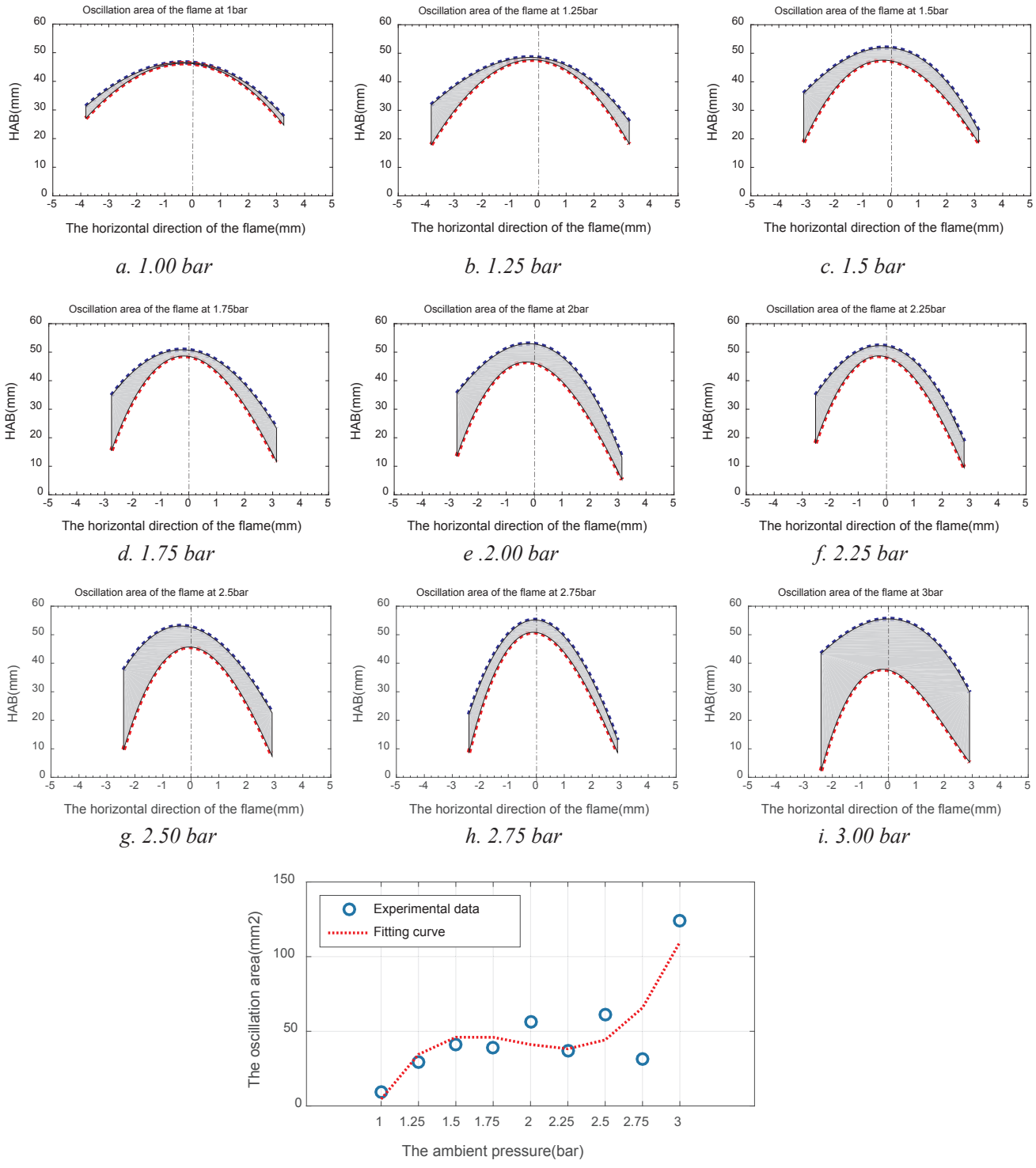

Fig. 3. Oscillation profiles of the top borders (by fitting) of the flames at different pressures.

were used to evaluate the stability of the flame in terms of the oscillation area. With the increase of the pressure, the luminance of the flame is enhanced. This indicates that the increase of pressure was favorable for the formation of PAHs and soot. The fact that the brightest area had a downward moving trend implies that the rich position of PAHs and soot moved down with pressure. Five samples under the same conditions were collected and the height of the peak value of the flame was recorded and analyzed. As shown in Fig. 3, the oscillation area of the flame increased, indicating that the stability of the flame deteriorated with pressure. The Y-axis in Fig. 3a–i is the centerline of the fuel tip.

By fitting a curve through the experimental results at different pressures, it is observed that the amplitude of the oscillation area of the flame increases with the pressure (Fig. 3j). In Fig. 3, the blue and the red fitted dotted lines refer to the upper and lower envelope lines of the flame top boundary respectively. The flame swing range is enlarged radically at 3 bar, and Fig. 3j shows that the oscillation area increases by 2–3 times suddenly between a pressure of 2.75 and 3 bar. This

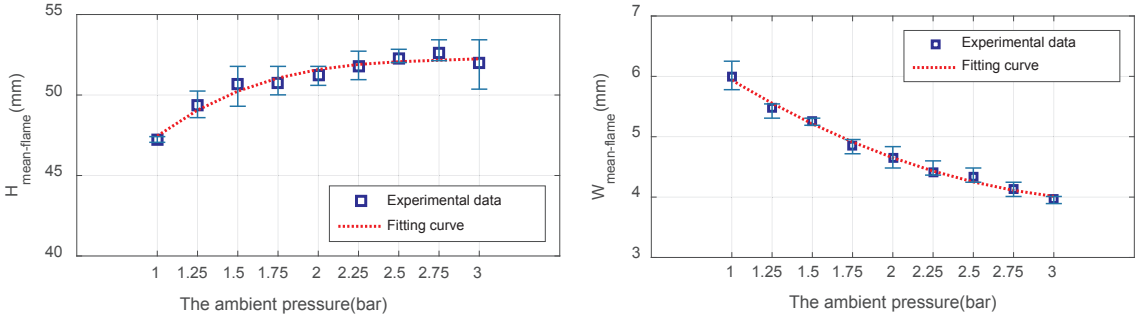

a. Mean height at different pressures *b. Mean width at different pressures*

Fig. 4. Variations of height and width of flames with pressures.

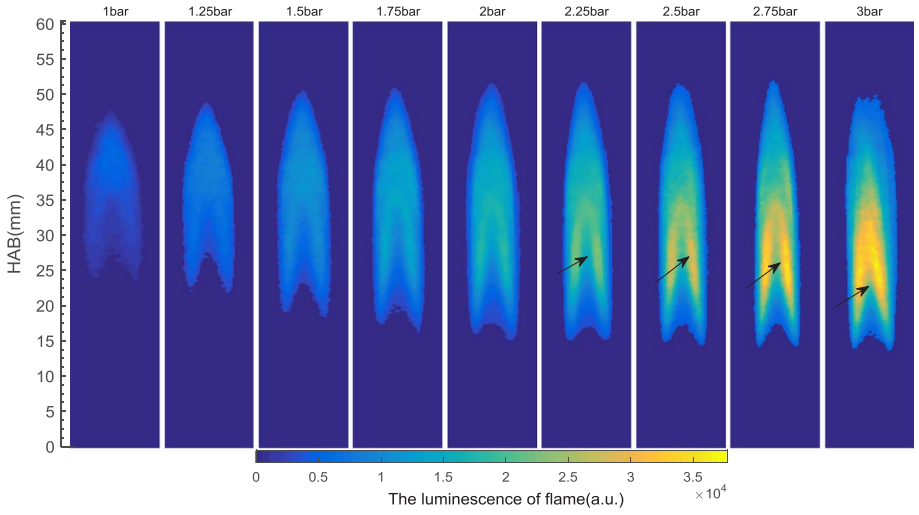

Fig. 5. A series of flame (LII + LIF) signals with pressure from 1.00 bar to 3.00 bar.

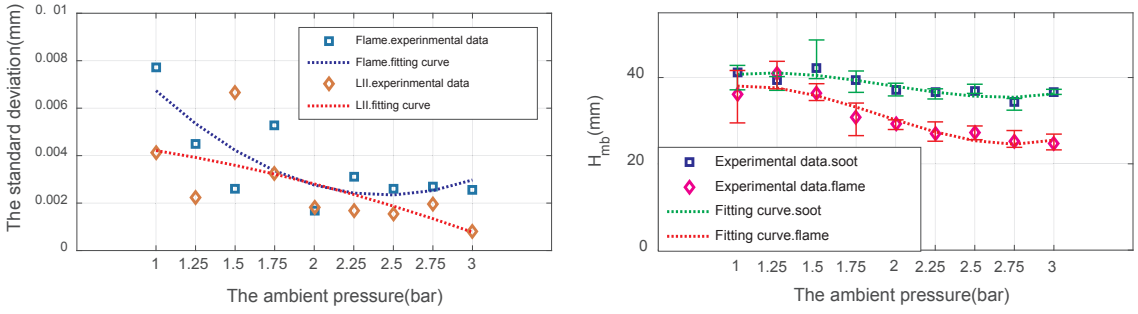

a. The standard deviation *b. The fitting curves*

Fig. 6. The height of brightest points (flame luminescence and LII-soot) of flame at different pressures.

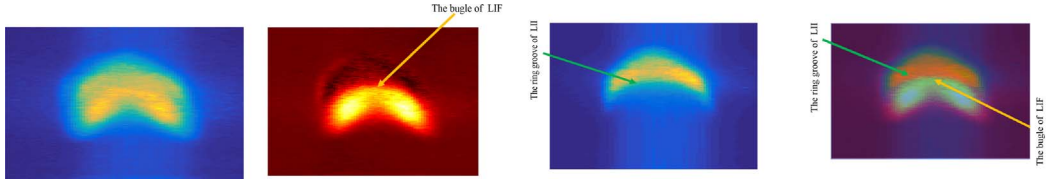

a. flame luminescence *b. PAH-LIF* *c. Soot-LII* *d. PAH-LIF and Soot-LII*

Fig. 7. The distribution of the PAH-LIF and Soot-LII on the flame (at 2.0 bar).

suggested that a further increase of the pressure would not feasible.

Moreover, the relationship between the pressure and the height or the width of the flame have been established in Fig. 4. The $H_{mean\text{-}flame}$ is the mean height of the flame and the $W_{mean\text{-}flame}$ is the mean width of the flame at different pressures. It shows that with the increase of pressure the flame becomes slender and slightly longer.

This figure demonstrates that the height of flame is little prone to be affected by pressure. When the pressure is above 1.5 bar, the height of

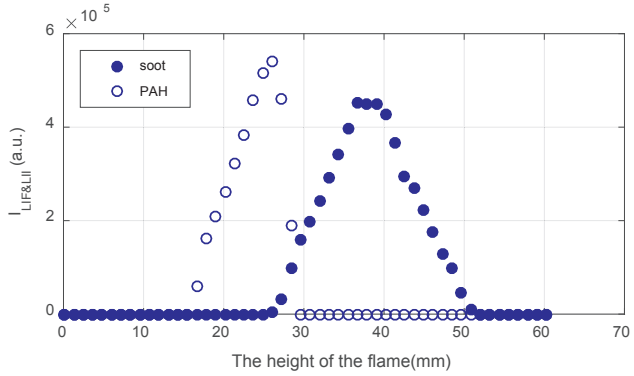

Fig. 8. The integrated intensity of soot and PAHs at different HABs (at 2 bar).

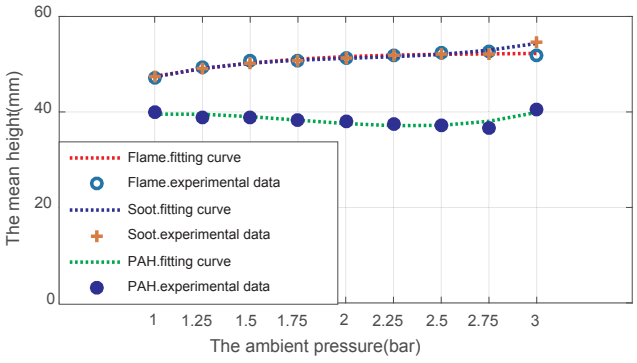

Fig. 9. The mean maximum height of flame, soot and PAHs at different pressures.

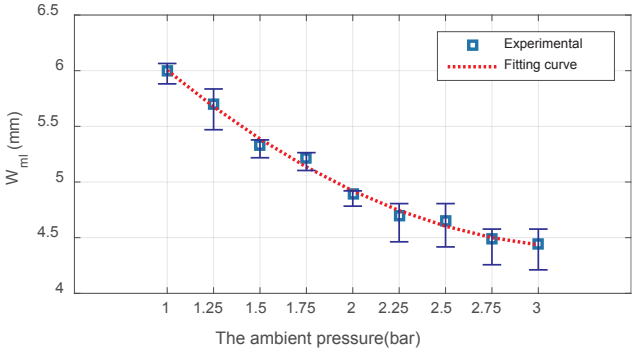

Fig. 11. The mean width of the LII signal at different pressure.

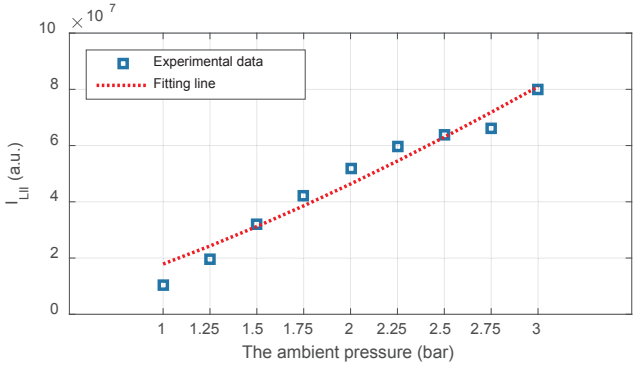

Fig. 12. The integrated intensity of LII signal at different pressure.

the flame is nearly constant. This is in line with results of F. G. Roper [24,25]. The slightly growing height of the flame only occurs between 1 bar and 1.5 bar, which might be a particular characteristic of the laminar diffusion flames of the liquid fuel [3]. As is shown in Fig. 5 for the LII plus LIF signals of the flames (de-noising is processed from the original data which can be found in the Supplementary material), two tails of the flame extended downwards, and the width of flame is slightly narrower. Moreover, the brightest area of the flames moved downward (indicated by the black arrows in Fig. 5).

The standard deviation of the height of the flame (the brightest point) has a tendency to decrease with pressure as well, as seen in Fig. 6a. Fig. 6b shows the variations of the height of the brightest points in the flame luminescence and LII with the pressure.

The H_{mb} is the mean height of the brightest point of flame luminescence or LII signals in Fig. 6b. In principle, this figure shows that the oscillations of the height of the brightest flame luminescence point are smaller than that of soot formation signals (as shown in the Fig. 6c for the standard deviations). It is speculated that the space the large and bright PAHs or soot particles occur and the distance between them might be compressed due to the gas density increased with the pressure, although the area of the PAHs and soot is also enlarged with the increase of pressure. As pressure increases, gaseous molecules become more closely packed, and thereby, the probability of a collision increases [26]. It will contribute to the more soot formation as a result of the larger probability of agglomeration and coalescence. At the same time, the temperature gradients were increased more heat is conducted to the flame core from the hot regions [26,27]. Great gradient of temperature near the burner exit enhances the thermal diffusion from the hot regions toward the center, which increases high fuel pyrolysis rate

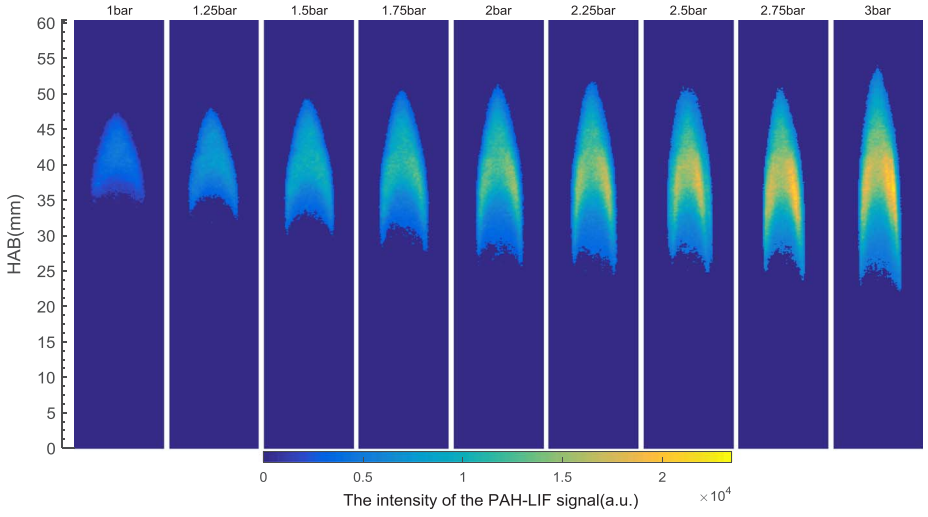

Fig. 10. Soot formation (LII Signal) images with pressure from 1.00 bar to 3.00 bar.

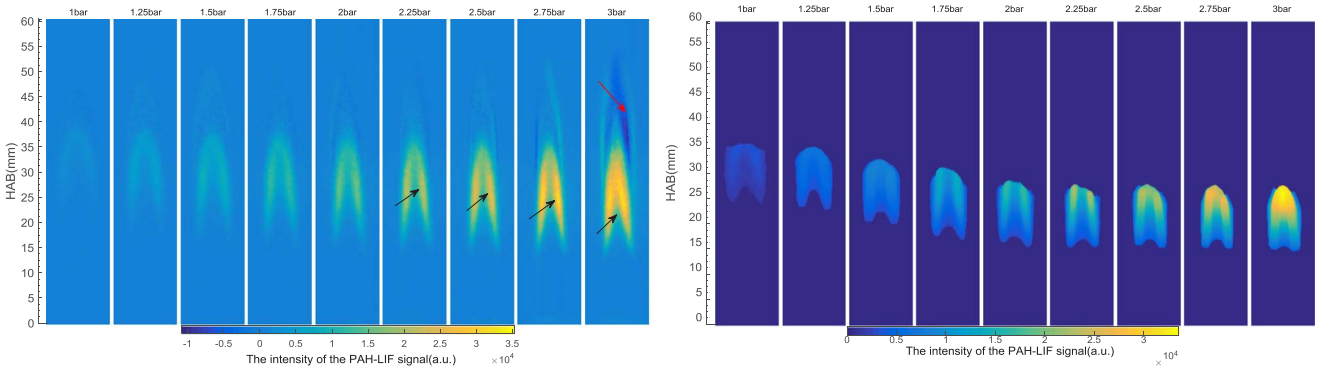

Fig. 13. PAHs formation of n-heptane flame (1.00 bar to 3.00 bar).

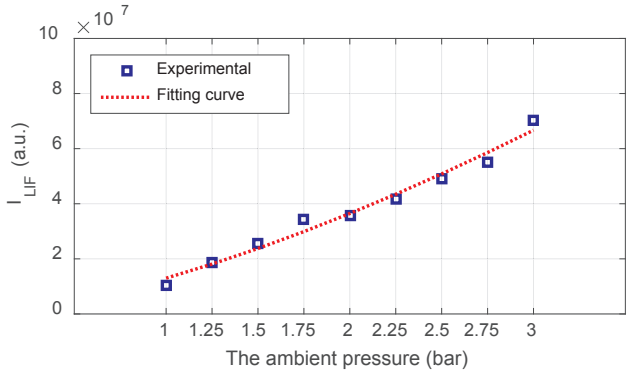

Fig. 14. Integrated Intensity of PAHs (1.00 bar to 3.00 bar).

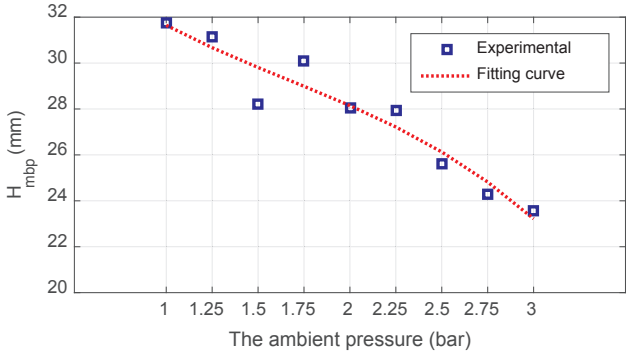

Fig. 15. The mean height of the brightest point of PAHs formation at different pressures.

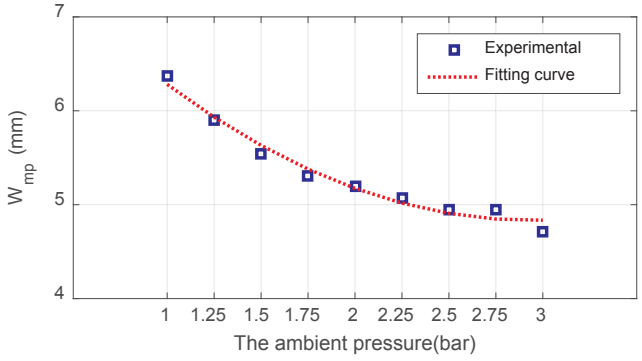

Fig. 16. The mean width of PAHs distribution at different pressures.

and accelerates PAHs formation and soot nucleation and growth as the pressure increases [27].

Compared with the luminescence signals, the lifetime of fluorescence signals of the PAHs is relatively shorter. Most of the fluorescence signals attenuated after 100 ns, which may lead to ascensions of the brightest points. It also suggests that the position of PAHs is formed at the lower part of the flame.

3.2. Soot formation

As shown in Fig. 7, the distribution of the PAHs signal was largely surrounded by the distribution of the soot signal and the bugle of PAHs area nearly fit inside the ring groove of soot signal.

The intensity of LIF signal, namely, PAHs concentration increased at first and then decreased, followed by soot concentration gradual increase (Fig. 8). As shown in Fig. 8 (The $I_{LIF\,\&\,LII}$ is the intensity of PAH-LIF or soot-LII), the PAHs formation signal was stronger at the lower part of the flame, it indicates that the PAHs is firstly created during the combustion and then reacted to generate soot, which was in line with the aforementioned observation. It proves that PAHs is the precursor of soot.

As shown in Fig. 9, the maximum height of soot almost coincided with the visible flame height, and the highest position of LIF-PAH signal was below that of the LII-soot signal. It demonstrates that the soot is the production of combustion rather than PAHs that escaped from the flame so that the soot distributed in the upper part of the flame. Furthermore, they are separated from each other at 3 bar caused by the unstable flame.

Due to the different lifetime of the fluorescence from excited PAHs and the incandescence from excited soot, the LII signal can be separated by a delay measurement. As shown in Fig. 10, the intensity of the soot formation increases dramatically with the pressure. Similarly, de-noising is processed and the original data can be found in Supplementary materials. The soot formation signal becomes slender, so that the width of soot signal becomes narrower, almost like a quadratic curve (The W_{ml} is the width of the soot formation signals in Fig. 11).

From Fig. 10, the soot formation signal expands up and down and the area of soot formation becomes larger while the pressure was elevated. The integrated soot formation intensities are shown in Fig. 12. It demonstrates that the soot formation rate nearly scales with $p^{1.38 \pm 0.32}$ with a 95% confidence bound. In the experiment of McCrain et al. [7], the region of peak f_v (soot volume fraction) shifted from the wings of the flame to the tip with increasing pressure for both methane–air and ethylene–air flames. However, for the liquid fuel of n-heptane, the brightest area, namely, the region of peak f_v was kept at a constant height in the flame and was more close to the centerline of the flame.

Moreover, Fig. 10 illustrates that regions with weak soot formation

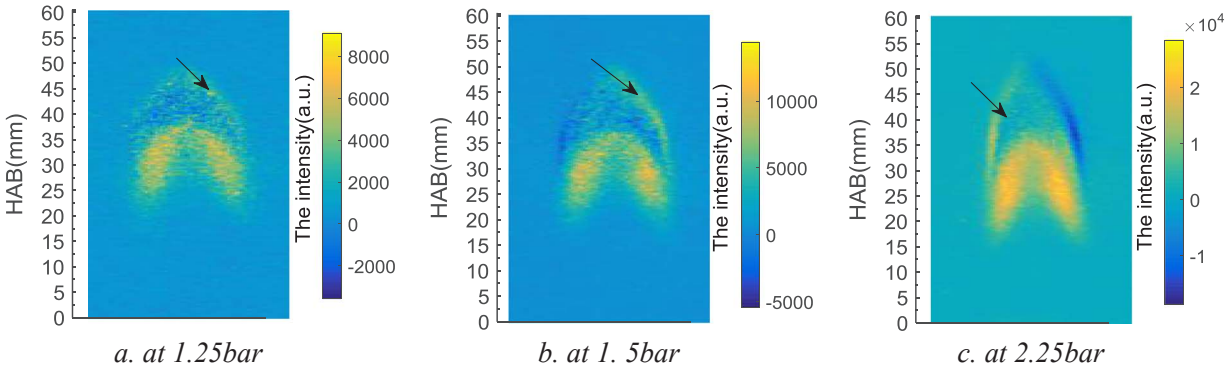

Fig. 17. PAHs distributions.

are surrounded by the strong soot formation signal. In addition, the intensity of left part of soot formation seems to be weaker than the right, suggesting that soot is absorbed by the laser in some way (e.g. sublimation), because the laser penetrates the flame from the right of the flame (see Fig. 1). This phenomenon is also found in previous research on soot formation, although the scale of target soot is different by LII with infrared laser (1064 nm) [3].

3.3. PAHs formation

Fig. 13 shows a series of PAH-LIF graphs for varying pressure from 1 to 3 bar. The PAHs intensity becomes negative in some areas (indicated by the red arrows in Fig. 13a). The negative values occur while the signal areas do not overlap each other accurately between two measurements due to the instability of the flames at specified condition. The negative area is obviously enlarged with pressure, which is evidence that the flame becomes unstable with pressure. The negative area becomes a bit larger suddenly at 3 bar, which proves that the flame stability may not be guaranteed if the pressure is above 3 bar. The net PAHs distribution after the post-processing (mentioned in Fig. 2) is shown in Fig. 13b.

The concentration of PAHs is increased with pressure is shown in Fig. 14 (The I_{LIF} is the intensity of the PAH-LIF signal). Similar to the soot formation, there exists a power law relationship between the integrated PAHs intensity and the ambient pressure, it scales with $p^{1.49 \pm 0.25}$ with a 95% confidence bound.

This demonstrates that the PAHs formation area is compressed with pressure, so that the height and width of the PAHs formation area moved downward and narrowed (as shown in Figs. 15 and 16). The H_{mbp} is the mean height of brightest point in PAHs signals in Fig. 15 and the W_{mp} is the mean width of the PAHs signals in Fig. 16.

The earlier formed PAHs which is located around the centerline of the flames with relatively lower temperature might be carbonized later and retained slightly longer than the PAHs formed in the periphery region [4,28,29]. As a result, there exists a ring distribution of the PAHs signals in the lower part of the flame, because the retained PAHs signals in the center area have been subtracted in this experiment (as indicated by the black arrows in Fig. 13a).

According to Bejaoui's research [14], relatively large PAHs will be excited by the laser of 532 nm and emits fluorescence. The first PAHs that appears above the burner tip has a smaller scale (2–3 rings) [30,31], then it gradually aggregates into larger PAHs whose position is elevated in the flame. A laser with a wavelength of 266 nm will excite the small size PAHs, which will be concentrated in the lower part of the flame near the burner tip [31]. An et al. found that PAHs could exist in gaseous phase and solid phase and PAHs of four or five rings could be attached to the soot particles [32]. This explains why there is a weak PAHs signal (indicated by the black arrows in the Fig. 17) in the main soot-LII signal distribution area above the distribution of the main PAH-LIF signal.

Besides, although the timing for capturing Image II is approaching the attenuation time of the initial soot formation of the flame, the small scale soot might be attenuated only partly and mixed with the PAHs. It assumed that this "impurity" does not interfere the detection of PAH-LIF signal which is dominated in the flame profile.

4. Conclusions

The measurements of PAHs formation have been carried out on laminar diffusion flames burning liquid n-heptane fuel. Although the flame stability deteriorated with increasing pressures, the measurement of PAHs and soot formation in laminar diffusion flames of n-heptane could be realized up to 3.0 bar with an appropriate design of the burner and fueling system. As the pressure increased from 1.0 to 3.0 bar, both the integrated intensity of PAHs and soot detected by the laser of 532 nm wavelength exhibited e a power law relationship with the pressure. The intensities of the PAHs and soot scaled with $p^{1.49 \pm 0.25}$ and $p^{1.38 \pm 0.32}$ respectively.

With the increase of pressure, both the distribution areas of the soot and PAHs moved downward and became slightly thinner towards the central area of the flame. In the lower parts of the soot and PAHs formation areas, the strong signals of soot and PAHs tend to form ring regions. Moreover, the distribution of the PAHs signal was largely surrounded by the distribution of the soot signal and the bugle of PAHs area nearly fit inside the ring groove of soot signals. The measurement of flame with more advanced laser diagnostics and the explorations about the mechanisms of PAHs formation are worth studying in future endeavors.

Acknowledgments

The authors thank the financial support from Shenzhen Science and Technology Innovation Committee (NO. JCYJ20160318094727251). The authors wish to acknowledge Dr. Nico Dam from Eindhoven University of Technology, for his support with the measurements. The authors also thank Dr. Zhiwei Sun from Centre for Energy Technology at the University of Adelaide in Australia, for his valuable suggestions and discussions.

Appendix A. Supplementary data

Supplementary data associated with this article can be found, in the online version, at http://dx.doi.org/10.1016/j.fuel.2017.07.074.

Reference

[1] Ravindra K, Sokhi R, Grieken RV. Atmospheric polycyclic aromatic hydrocarbons: source attribution, emission factors and regulation. Atmos Environ 2008;42:2895–921.
[2] Liu B, Xue ZQ, Zhu XL, Jia CR. Long-term trends (1990–2014), health risks, and sources of atmospheric polycyclic aromatic hydrocarbons (PAHs) in the U.S.

Environ Pollut 2017;220:1171–9.
[3] Zhou L, Dam NJ, Boot MD, De Goey LPH. Measurements of sooting tendency in laminar diffusion flames of n-heptane at elevated pressure. Combust Flame 2013;160:2507–16.
[4] Vander Wal RL. Investigation of soot precursor carbonization using laser-induced fluorescence and laser-induced incandescence. Combust Flame 1997;110:281–4.
[5] Eaves NA, Veshkini A, Riese C, Zhang Q, Dworkin SB, Thomson MJ. A numerical study of high pressure, laminar, sooting, ethane–air coflow diffusion flames. Combust Flame 2012;159:3179–90.
[6] Slavinskaya NA, Frank P. A modelling study of aromatic soot precursors formation in laminar methane and ethene flames. Combust Flame 2009;156:1705–22.
[7] McCrain LL, Roberts WL. Measurements of the soot volume field in laminar diffusion flames at elevated pressures. Combust Flame 2005;140:60–9.
[8] Joo H, Gülder ÖL. Experimental study of soot and temperature field structure of laminar co-flow ethylene–air diffusion flames with nitrogen dilution at elevated pressures. Combust Flame 2011;158:416–22.
[9] Thomson KA, Gülder ÖL, Weckman RA, Fraser EJ, Smallwood GJ, Snelling DR. Soot concentration and temperature measurements in co-annular, nonpremixed CH_4/air laminar flames at pressures up to 4 MPa. Combust Flame 2005;140:222–32.
[10] Mandatori PM, Gülder ÖL. Soot formation in laminar ethane diffusion flames at pressures from 0.2 to 3.3 MPa. Proc. Combust. Inst. 2011;33:577–84.
[11] Jin HF, Frassoldati A, Wang YZ, Zhang XY, Zeng MR, Li YY, et al. Kinetic modeling study of benzene and PAH formation in laminar methane flames. Combust Flame 2015;162:1692–711.
[12] Gülder ÖL, Intasopa G, Joo HI, Mandatori PM, Bento DS, Vaillancourt ME. Unified behaviour of maximum soot yields of methane, ethane and propane laminar diffusion flames at high pressures. Combust Flame 2011;158:2037–44.
[13] Bento DS, Thomson KA, Gülder ÖL. Soot formation and temperature field structure in laminar propane–air diffusion flames at elevated pressures. Combust Flame 2006;145:765–78.
[14] Bejaoui S, Mercier X, Desgroux P, Therssen E. Laser induced fluorescence spectroscopy of aromatic species produced in atmospheric sooting flames using UV and visible excitation wavelengths. Combust Flame 2014;161:2479–91.
[15] Daca AE, Gülder ÖL. Soot formation characteristics of diffusion flames of methane doped with toluene and n-heptane at elevated pressures. Proc Combust Inst 2017;36:737–44.
[16] Andrade Oliveira MH, Olofsson NE, Johnsson J, Bladh H, Lantz A, Li B, et al. Soot, PAH and OH measurements in vaporized liquid fuel flames. Fuel 2013;112:145–52.
[17] Andrade Oliveira MH, PhD Thesis, Eindhoven University of Technology, 2012.
[18] Viteri F, Salinas J, Millera Á, Bilbao R, Alzueta MU. Pyrolysis of dimethyl carbonate: PAH formation. J Anal Appl Pyrol 2016;122:524–30.
[19] An YZ, Li X, Teng SP, Wang K, Pei YQ, Qin J, et al. Development of a soot particle model with PAHs as precursors through simulations and experiments. Fuel 2016;179:246–57.
[20] Melton A. Soot diagnostics based on laser heating. Appl Opt 1984;23:2201–8.
[21] Quay B, Lee TW, Ni T, Santoro RJ. Spatially resolved measurements of soot volume fraction using laser-induced incandescence. Combust Flame 1994;97:384–92.
[22] Ossler F, Metz T, Alden M. Picosecond laser-induced fluorescence from gas-phase polycyclic aromatic hydrocarbons at elevated temperatures. Appl. Phys. B 2001;72:465–78.
[23] Verhoeven LM, Andrade Oliveira MH, Lantz A, Li B, Li ZS, Luijten CCM, et al. A numerical and experimental study of polycyclic aromatic hydrocarbons in a laminar diffusion flame. Proc. Combust. Inst. 2013;34:1819–26.
[24] Roper FG. The prediction of laminar jet diffusion flame sizes: part I. Theor. Model Combust. Flame 1977;29:219–26.
[25] Roper FG, Smith C, Cunningham AC. The prediction of laminar jet diffusion flame sizes: part II. Exp. Verification 1977;29:227–34.
[26] Karatas AE, Gülder ÖL. Soot formation in high pressure laminar diffusion flames. Prog Energy Combust Sci 2012;38:818–45.
[27] Li S. Modeling of pressure effects on flame structure and soot formation of n-heptane/air co-flow laminar flames by skeletal reaction mechanism. Appl Therm Eng 2016;106:1458–65.
[28] Kholghya M, Saffaripoura M, Yipb C, Thomson JM. The evolution of soot morphology in a laminar coflow diffusion flame of a surrogate for Jet A-1. Combust Flame 2013;160:2119–30.
[29] Haynes BS, Wagner HG. Progress and development of energy and combustion. Science 1981;7:229–73.
[30] Wu JT, Song KH, Litzinger T, Lee SY, Santoro R, Linevsky M, et al. Reduction of PAH and soot in premixed ethylene–air flames by addition of ethanol. Combust Flame 2006;144:675–87.
[31] Chen B, Liu XL, Liu HF, Wang H, Kyritsis DC, Yao MF. Soot reduction effects of the addition of four butanol isomers on partially premixed flames of diesel surrogates. Combust Flame 2017;177:123–36.
[32] An YZ, Teng SP, Pei YQ, Qin J, Li X, Zhao H. An experimental study of polycyclic aromatic hydrocarbons and soot emissions from a GDI engine fueled with commercial gasoline. Fuel 2016;164:160–71.